AN ANALYSIS OF FATIGUE CRACK GROWTH UNDER YIELDING CONDITIONS

M. W. Brown*, H. W. Liu**, A. P. Kfouri*, K. J. Miller*

*Dept. Mech. Engng., Sheffield Univ., Mappin Street, Sheffield, S1 3JD, UK
**Dept. Chem. Engng. & Mat. Sci., Syracuse Univ., Syracuse, New York 13210, USA

ABSTRACT

The local stress strain field at a crack tip under either general yielding (fully plastic loading) or small scale yielding conditions may be characterized by a single parameter. In situations where there is no size effect the rate of fatigue crack propagation is shown to be proportional to this parameter, which is called the severe strain zone size. The predicted behaviour is compared with not only empirical data for 1018 steel, from low cycle strain controlled fatigue tests at room temperature, but also with a crack growth law applicable to low stresses within the limitations of linear elastic fracture mechanics. The severe strain zone size is determined from an elastic-plastic finite element analysis of the crack tip stress strain field.

KEYWORDS

Fatigue; crack propagation; mild steel; stress analysis; finite element analysis; plastic zone size; crack opening displacement; crack tip.

INTRODUCTION

Research into fatigue crack propagation (FCP) bas been concerned mainly with situations where the applied stress is well below the yield stress, giving small scale yielding conditions (SSY). In this case linear elastic fracture mechanics (LEFM) may be used to characterize the local stress and strain fields around the tip of a growing crack, so that FCP laws can be formulated in terms of the stress intensity factor, K. However a few experimental studies (Hammouda, 1978; Solomon, 1972; Solomon, 1973; Wareing, 1975) have considered crack growth under fully plastic conditions in strain controlled tests, where cracks behave similarly to those in conventional low cycle fatigue situations. When crack tip plasticity is extensive, K is not a suitable parameter for describing FCP. Therefore Solomon (1972) has derived an empirical correlation for cracking in a thin plate of 1018 steel at room temperature,

$$da/dN = 11.4\ (\Delta\varepsilon_{zp})^{1.86}\ a \qquad (1)$$

where a is crack length, N the number of cycles and $\Delta\varepsilon_{zp}$ the transverse plastic strain range. The same type of equation has been used for A286 (Solomon, 1973), mild steel (Hammouda, 1978) and two stainless steels (Wareing, 1975). It may also represent Stage I FCP in torsional tests for mild steel (Ibrahim and Miller, 1980) and 1% Cr-Mo-V steel (Miller and Gardiner, 1977).

A theoretical crack growth rule is derived in the present paper, applicable to both SSY and general yielding conditions, giving predictions which are compared to the experimental data.

CRACK TIP STRESS STRAIN FIELD

Hu and Liu (1976) have produced evidence that for plane stress conditions the stresses and strains near the tip of a crack may be characterized by a single parameter, which they have taken to be the plastic zone size. The same conclusion was reached by Kuo and Liu (1976) for plane strain. Since the concept of a plastic zone can have no physical meaning under general yield, Hu and Liu proposed an extrapolation procedure, outlined below, in order to define a characteristic dimension analogous to the plastic zone size. This characterizes the crack tip conditions by using the equations developed for SSY. In the present work we specifically define this dimension as the size of a zone of 'severe strain' r_s.

This concept may be introduced into FCP models by appealing to dimensional analysis. When conditions are such that there are no size effects, which may arise from specimen geometry or microstructural features, the crack extension in a single fatigue cycle is determined by the local stresses and strains at the crack tip. As stresses and strains are uniquely described by the parameter r_s, together with various material properties such as the cyclic stress strain curve, we may postulate, typically, that

$$da/dN = f(r_s, n, E, k, \varepsilon_f)$$

where n is the cyclic strain hardening exponent, E Young's modulus, k the cyclic strength coefficient and ε_f the true fracture ductility. From dimensional analysis, we find that

$$(da/dN)/r_s = \kappa \qquad (2)$$

where κ is a dimensionless material-dependent constant, being a function of the above material properties. Equation (2) will not apply when microstructural features such as grain size have a significant influence on the crack propagation rate.

Under SSY conditions, r_s is identical to the plastic zone size, being equal to $\alpha(K/\sigma_y)^2$ where α is a constant and σ_y is the yield stress. If K is replaced by ΔK, equation (2) reduces to the Paris law for FCP with an exponent of 2 on ΔK which is in agreement with a number of proposed mechanisms where crack extension has been related to plastic zone size (Plumbridge, 1972). The equivalence of plastic zone sizes for similar crack growth rates has also been demonstrated by Miller (1977) in correlating data under different biaxial stress states.

FINITE ELEMENT ANALYSIS

In order to assess the validity of equation (2) under general yielding, an elastic-plastic finite element study was undertaken using a specimen geometry similar to Solomon's. The programme based on the initial stress approach has been used in a number of previous analyses, e.g. Kfouri and Miller (1976). The finite element idealization of the specimen is shown in Fig. 1. Plane stress conditions were assumed, and the lateral curvature was simulated by layers of varying thickness as illustrated. The material obeyed the von Mises criterion but the stress strain curve was modelled on Solomon's results, with an assumed yield behaviour characteristic of mild steel, and strain hardening given by the Ramberg-Osgood equation (Fig. 2),

$$\sigma = k(\varepsilon_p)^n$$

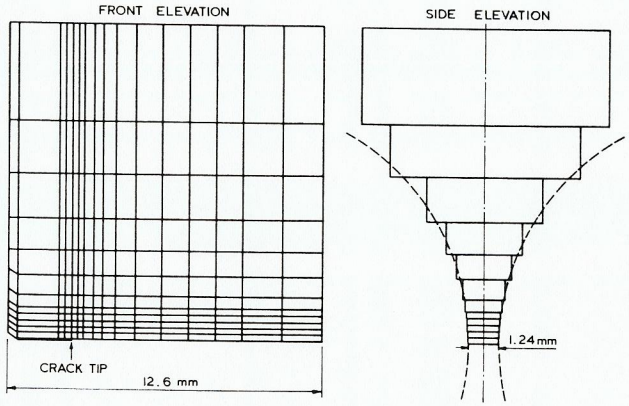

Fig. 1. Finite element idealization for Solomon's specimen, showing top half and cross section (a = 2.54 mm).

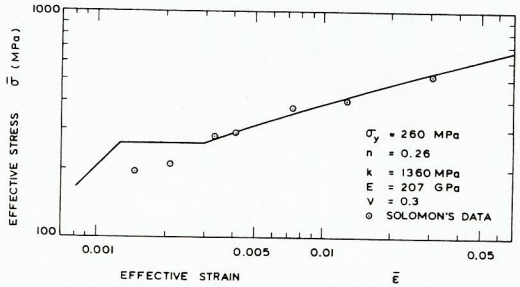

Fig. 2. Stress strain curve.

Cases involving three crack lengths were analysed covering the range observed in Solomon's experiments. The applied load P was adjusted automatically to P_o, which was 95% of the load required to cause incipient yielding at the crack tip node, and then incremented by steps of 0.08 P_o.

For different load values the distribution of effective stress, $\bar{\sigma}$, ahead of the crack tip may be plotted as in Fig. 3. This shows that where the material deforms plastically the crack tip singularity has a characteristic slope of -0.119, which was common to each crack analysed. In Fig. 4, these results have been replotted to obtain a single line for the near tip behaviour by normalizing the stress with yield stress and the distance from the crack tip, r, with r_s. The severe strain zone size is determined in Fig. 3, being the intercept of the line of slope -0.119 with the yield stress, this line being extrapolated as required.

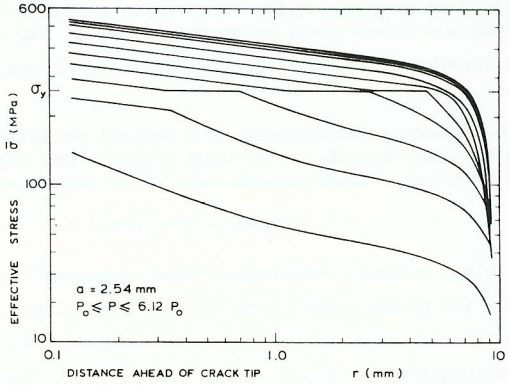

Fig. 3. Equivalent stress ahead of crack tip with increasing load.

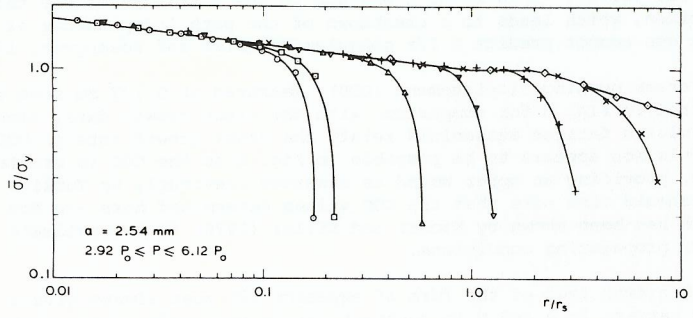

Fig. 4. Normalized stress distribution.

Similarly one may plot the strain distribution which gives a slope of -0.500 for any component of strain which may be considered. Fig. 5 is a typical example, showing the tensile strain normal to the crack plane varying with distance ahead of the crack tip, where the line drawn through the data is actually the best fit for another case, i.e. a = 1.27 mm. The characteristic slopes will depend in general

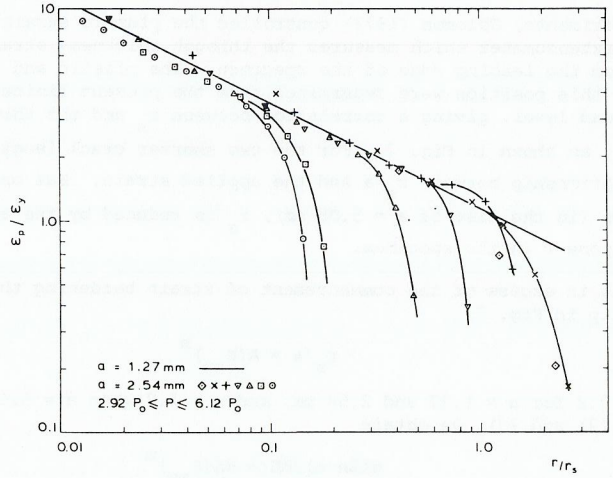

Fig. 5. Normalized plastic strain distribution for various loads.

on the strain hardening exponent, the loading conditions and specimen geometry (Hu and Liu, 1976; Kuo and Liu, 1976).

For the longest crack measured by Solomon in his experiments (a = 5.08 mm), a plastic hinge develops in the specimen, as shown in Fig. 6. In spite of this, the characteristic slopes determined at shorter crack lengths remain applicable.

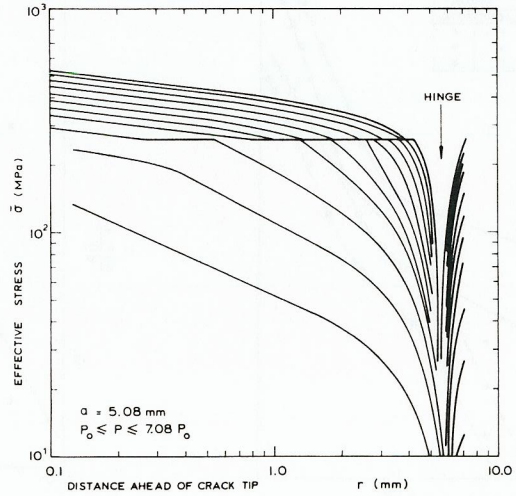

Fig. 6. Stress distribution for long cracks showing plastic hinge.

APPLICATION TO FATIGUE CRACK PROPAGATION

In his experiments, Solomon (1972) controlled the plastic strain range with a diametral extensometer which measured the through thickness strain at a point 7.62 mm from the leading edge of the specimen. The plastic and total strain components at this position were determined from the present finite element analysis for each load level, giving a correlation between r_s and the through thickness strain, ε_z, as shown in Fig. 7. For the two shorter crack lengths there is a single relationship between r_s/a and the applied strain. But once the plastic hinge forms (in the case of a = 5.08 mm), r_s is reduced by the additional bending strain component in the specimen.

For strains in excess of the commencement of strain hardening there is a power law relationship in Fig. 7,

$$r_s/a = A(\varepsilon_{zp})^m \tag{3}$$

where m = 2.2 for a = 1.27 and 2.54 mm, and m = 1.8 when a = 5.08 mm. Combining equations (2) and (3), we obtain

$$d(\ell n\ a)/dN = \kappa A(\varepsilon_{zp})^m \tag{4}$$

which is of the same form as equation (1), Solomon's empirical rule. There is a slight difference in the calculated exponent values, which may be due in part to the formation of the plastic hinge with a = 5.08 mm; note that the empirical exponent of 1.86 lies between the calculated values for m.

Fig. 8 shows a direct comparison of the empirical data with the finite element predictions according to equation (4), assuming $\varepsilon_{zp} = \frac{1}{2}\,\Delta\varepsilon_{zp}$ and taking $\kappa = 6 \times 10^{-5}$.

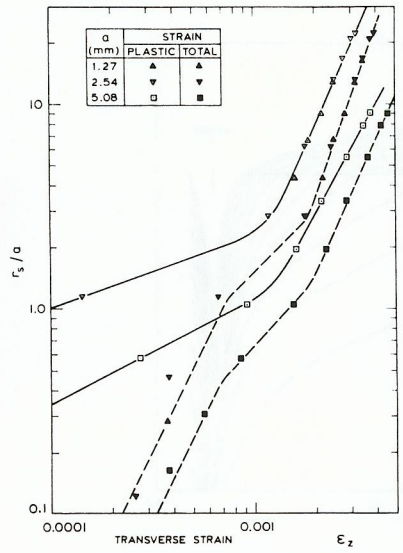

Fig. 7. Severe strain zone size dependence on applied strain.

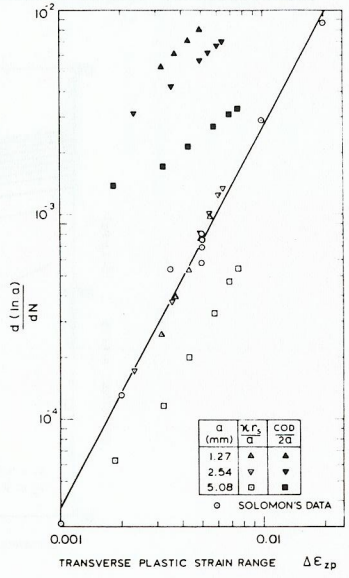

Fig. 8. Correlation of empirical crack growth data.

Clearly the finite element results lie within the scatter of test results over the range of strains analysed. As crack lengths become large ($\sim$ 5 mm), the predicted crack growth rate is reduced, which one would anticipate from the strain control method employed where the crack tip approaches the point of strain measurement. This reduction commences when 2.54 < a < 5.08 according to the finite element analysis, where the upper and lower halves of the specimen were permitted to rotate freely. However the use of button-head specimens by Solomon introduced some restraint against such rotation, delaying the predicted formation of a plastic hinge to longer crack lengths, presumably until a > 5.08 mm.

DISCUSSION

The concept of the severe strain zone size governing the rate of crack growth in fatigue is compatible with Solomon's results in Fig. 8, as long as the crack length is small compared to specimen width (12.6 mm). Should a full finite element analysis include the button-head gripping system, r_s may also be able to correlate FCP for crack lengths up to 5 mm, if the influence of specimen width is small in equation (2).

The constant κ determined empirically for general yielding conditions should also be applicable to crack growth in the LEFM regime. One may test this assumption approximately by using a crack growth rule (Pook and Frost, 1973), such as

$$da/dN = 9/\pi.(K/E)^2 \tag{5}$$

applicable to plane stress conditions. From equations (2) and (5), and noting that $r_s = (K/\sigma_y)^2/2\pi$ for plane stress (see above), one finds $\kappa = 18(\sigma_y/E)^2$, or 2.8×10^{-5} for the stress strain curve in Fig. 2. This compares well with the empirical value of 6×10^{-5}, although other crack growth laws may give less favourable values for κ.

The stress-strain analysis gives a somewhat surprising result in that the sum of the characteristic slopes for the stress and strain distribution respectively (0.619) is not equal to unity, contrary to the results of Hu and Liu (1976) and Kuo and Liu (1976). This is probably due to the variation of the thickness of the specimen, which leads to a breakdown of the path independence of the J-integral, so that one cannot predict a 1/r singularity (Rice and Rosengren, 1968).

The crack opening displacement (COD), measured at 0.127 mm from the crack tip, is plotted in Fig. 8 for comparison with the crack growth data, since a number of postulated fatigue mechanisms relate the crack growth rate to COD/2. No such correlation appears to be possible in Fig. 8 as the COD is greater than the growth rate, providing an upper bound as observed previously by Tomkins (1975). However one should also note that the COD values determined here are for static loading, which has been shown by Kfouri and Miller (1976) to overestimate the COD obtained under propagating conditions.

Crack growth laws of the form of equation (2) must always give a linear relationship between ℓn a and N in constant strain amplitude tests, since r_s is proportional to a when there is no size effect. Straight line graphs of ℓn a plotted against N have been demonstrated using various metals over a wide range of strain ranges under both plastic loading (Hammouda, 1978; Solomon, 1973; Wareing, 1975) and elastic loading (Frost, 1959; Liu, 1961) conditions. The present work has enabled the concept of plastic zone size to be extended to cover both of the regimes with a simple crack growth rule. One may extend this approach to the work of Wareing (1975) and Hammouda (1978), both of whom used an edge cracked specimen

of square cross section, but the finite element analysis employed to determine r_s must relate to plane strain conditions.

CONCLUSIONS

An equation for fatigue crack growth rate has been derived from dimensional analysis which is applicable to both small scale yielding and general yielding conditions. The predictions compare well with experimental results for 1018 steel.

REFERENCES

Frost, N. E. (1959). Propagation of fatigue cracks in various sheet materials. J. Mech. Engng. Sci., 1, 151-170.

Hammouda, M. M. I. (1978). Fatigue crack initiation at notches. Ph.D. Thesis, University of Cambridge.

Hu, W. and Liu, H. W. (1976). Characterization of crack tip stresses and strains - small scale yielding and general yielding. Proc. 2nd Int. Conf. Mechanical Behaviour of Materials, Boston, pp. 1058-1062.

Ibrahim, M. F. E. and Miller, K. J. (1980). Determination of fatigue crack initiation life. Fatigue Engng. Mater. Struct., 2.

Kfouri, A. P. and Miller, K. J. (1976). Crack separation energy rates in elastic-plastic fracture mechanics. Proc. Instn. Mech. Engrs., 190, 571-584.

Kuo, A. S. and Liu, H. W. (1976). An experimental and FEM study on crack opening displacement and its application to fatigue crack growth. Syracuse Univ. Rep. No. MTS-HWL-F-1076.

Liu, H. W. (1961). Crack propagation in thin metal sheet under repeated loading. Trans. ASME Ser. D., 83, 23-31.

Miller, K. J. and Gardiner, T. (1977). High temperature cumulative damage for stage I crack growth. J. Strain Analysis, 12, 253-261.

Miller, K. J. (1977). Fatigue under complex stress. Metal Science, 11, 432-438.

Plumbridge, W. J. (1972). Review: Fatigue-crack propagation in metallic and polymeric materials. J. Mater. Sci., 7, 939-962.

Pook, L. P. and Frost, N. E. (1973). A fatigue crack growth theory. Int. J. Fracture, 9, 53-61.

Rice, J. R. and Rosengren, G. F. (1968). Plane strain deformation near a crack tip in a power law hardening material. J. Mech. Phys. Solids, 16, 1-12.

Solomon, H. D. (1972). Low cycle fatigue crack propagation in 1018 steel. J. Mater., 7, 299-306.

Solomon, H. D. (1973). Frequency dependent low cycle fatigue crack propagation. Met. Trans., 4, 341-347.

Tomkins, B. (1975). The development of fatigue crack propagation models for engineering applications at elevated temperatures. Trans. ASME Ser. H., 97, 289-297.

Wareing, J. (1975). Fatigue crack growth in a type 316 stainless steel and a 20% Cr/25% Ni/Nb stainless steel at elevated temperature. Met. Trans., 6A, 1367-1377.